High-coercivity Dy - Fe - X (X = C, B) alloys made by mechanical alloying

High-coercivity Dy–Fe–X (X = C, B) alloys made by mechanical alloying

Y C Sui†, Z D Zhang, Q F Xiao, W Liu, X G Zhao, T Zhao and Y C Chuang

Institute of Metal Research, Academia Sinica, Shenyang 110015, People's Republic of China, and International Centre for Material Physics, Academia Sinica, Shenyang 110015, People's Republic of China

Abstract. The structure, phase transformation and magnetic properties of mechanically alloyed (MA) samples of $Dy_m Fe_{92-m} Z_8$ (Z = C, B) ($13 \leqslant m \leqslant 20$) have been studied systematically. The tetragonal $Dy_2 Fe_{14} C$ compound can be formed within a wide composition range, $15 \leqslant m \leqslant 18$. When $m \geqslant 19$ or $m \leqslant 14$, $Dy_2 Fe_{17} C_x$ with different Curie temperatures forms accompanying the $Dy_2 Fe_{14} C$ phase. An fcc structure Dy-rich phase emerges during the annealing process and its amount increases with the increment of Dy content. The composition range for the formation of $Dy_2 Fe_{14} B$ is rather narrower than that of $Dy_2 Fe_{14} C$. When $m \geqslant 16$, $Dy_6 Fe_{23}$ is formed. When $m \leqslant 14$, a certain amount of α-Fe that is unreacted with Dy and C is left. No Dy-rich phase if found in the Dy–Fe–B series of alloys. The highest intrinsic coercivities obtained in Dy–Fe–C and Dy–Fe–B systems are 93 kOe and 70 kOe respectively.

1. Introduction

Coercivity as large as 27.5 kOe can be obtained in a $Dy_{13} Fe_{80} C_7$ casting after appropriate heat-treatment, which consists of separate $Dy_2 Fe_{14} C$ crystallites and does not contain magnetic domain walls [1]. Stadelmaier *et al* observed a coercivity value of 15 kOe in annealed $Dy_{15} Fe_{77} C_8$ polycrystalline samples in which $Dy_2 Fe_{14} C$ grains having diameters in the 1–10 μm range are surrounded by a thin intergranular layer with a composition close to that of the principal 2:14:1 phase [2]. $R_2 Fe_{14} X$ (R = $Nd_x Dy_{1-x}$; X = B, C or $B_x C_{1-x}$) samples made by Liu and Stadelmaier showed that coercivity higher than 12 kOe can be reached for the optimum composition range and it was claimed to be caused by a cellular microstructure with cell sizes about 1 μm [3]. So the Dy–Fe–C alloys provide some special metallurgical and microstructural features that do not simply duplicate the known materials. $Dy_{15} Fe_{77} B_8$ synthesized by mechanical alloying and subsequent annealing presented coercivity as high as 56 kOe [4]. $Dy_{13.5} Fe_{81.3} B_{5.4}$ alloy, which was rapidly solidified under an appropriate quenching rate without annealing, had a maximum coercivity value of 64 kOe [5]. Also appropriate Dy substitution has been widely and efficiently used in the manufacture of Nd–Fe–B magnets for the purpose of increasing coercivity. Dy concentration higher than $x = 0.47$ results in the formation of $DyFe_4 B$ along grain boundaries in the sintered $(Nd_{1-x} Dy_x)_{15} Fe_{77} B_8$ magnets and decreases the intrinsic coercivity [6]. In order to study the coercivity mechanism of the carbides and borides, in

† Correspondence address: Y C Sui, Institute of Metal Research, Academia Sinica, Shenyang 110015, People's Republic of China. E-mail address: wliu@imr.ac.cn
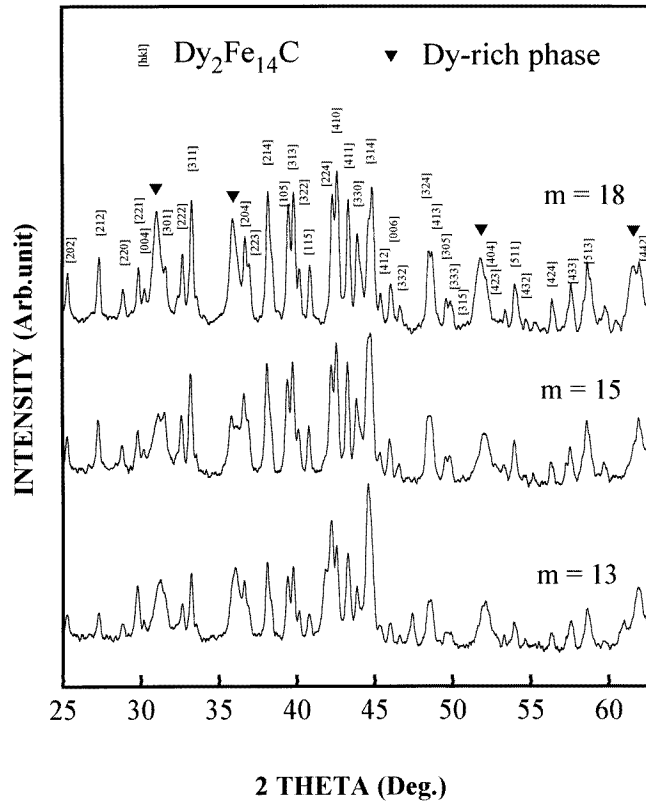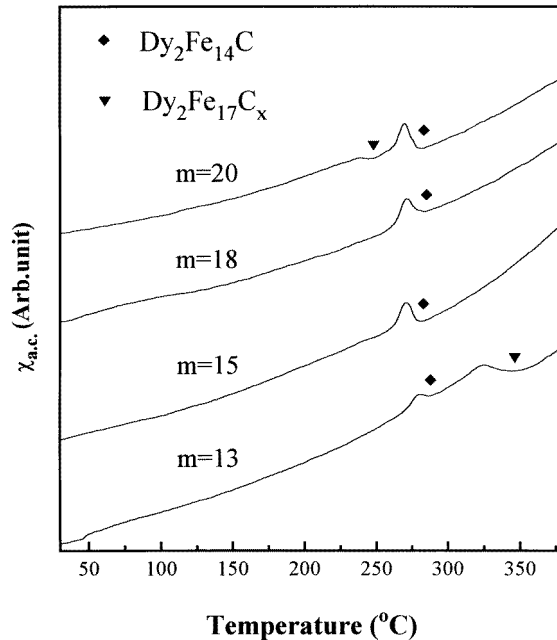
Figure 1. X-ray diffraction patterns of mechanically alloyed $Dy_m Fe_{92-m} C_8$ alloys annealed at 900 °C for 35 min.

this paper, mechanical alloying is employed to prepare alloys with $Dy_2Fe_{14}C$ or $Dy_2Fe_{14}B$ as matrix phases. Both the magnetic properties and the phase transformation processes are studied.

2. Experimental details

Samples of Dy–Fe–Z (Z = B, C) alloys were prepared from 99.99% pure Dy powder and 99.5% Fe powder, 99.7% pure carbon powders and 99% boron powder. The mechanical alloying was performed in an high-energy ball mill under pure argon atmosphere for 6 h. The mechanically alloyed powders were annealed in a vacuum furnace connected to a closed glove box in which sample preparation is carried out. X-ray diffraction analysis was conducted using Cu Kα radiation with a Rigaku D/max-ray diffractometer equipped with a graphite crystal monochromator. Dy–Fe–X (X = C, B) powders were embedded in epoxy resin to form bonded samples. Magnetic properties were measured using a pulsed field magnetometer in fields up to 12 T. The magnetization was related to the amount of magnetic powders, neglecting the dilution effect of resin and the density of the alloys was assumed to be 7.6 g cm^{-3}. AC initial susceptibility measurement was performed to determine Curie temperatures of the phases in the Dy–Fe–Z (Z = C, B) alloys.

Figure 2. χ_{ac} against temperature of mechanically alloyed $Dy_m Fe_{92-m} C_8$ alloys annealed at 900 °C for 35 min.

3. Results

3.1. Structure and phase transition

3.1.1. $Dy_m Fe_{92-m} C_8$ ($13 \leqslant m \leqslant 20$). Figures 1 and 2 respectively show x-ray diffraction patterns and χ_{ac}–temperature curves of MA $Dy_m Fe_{92-m} C_8$ alloys annealed at 900 °C for 35 min. Because the main x-ray diffraction peaks of $Dy_2 Fe_{17} C_x$ and $Dy_2 Fe_{14} C$ overlap each other, it is impossible to distinguish $Dy_2 Fe_{17} C_x$ from $Dy_2 Fe_{14} C$ by x-ray diffraction patterns only. The χ_{ac}–temperature curve is used conveniently to identify phases with different Curie temperatures in one alloy. It is found that $Dy_2 Fe_{14} C$ can be formed within a wide composition range of $15 \leqslant m \leqslant 18$. When $m \leqslant 14$ or $m \geqslant 19$, $Dy_2 Fe_{17} C_x$ is formed during the annealing process: Curie temperatures of $Dy_2 Fe_{17} C_x$ formed in $Dy_{13} Fe_{79} C_8$ and $Dy_{20} Fe_{72} C_8$ alloys are 340 and 250 °C respectively which means that the interstitial carbides of $Dy_2 Fe_{17} C_x$ formed in different alloys have different carbon concentrations [7]. There is an fcc Dy-rich phase with lattice parameter of $a = 4.98$ Å in the mechanically alloyed Dy–Fe–C alloys. Its amount increases with the increment of Dy content.

When the annealing temperature increases to 1000 °C, $Dy_2 Fe_{17} C_x$ still exists in the $m \leqslant 14$ and $m \geqslant 19$ alloys, but their Curie temperatures drop down a little compared with those in the same alloys annealed at 900 °C. This may be caused by the partial phase transformation from $Dy_2 Fe_{17} C_x$ to $Dy_2 Fe_{14} C$ which extracts the carbon from the remaining $Dy_2 Fe_{17} C_x$.

3.1.2. $Dy_m Fe_{92-m} B_8$ ($13 \leqslant m \leqslant 20$). Figures 3 and 4 respectively show x-ray diffraction patterns and χ_{ac}–temperature curves of MA $Dy_m Fe_{92-m} B_8$ alloys annealed at 900 °C for 35 min. Compared with $Dy_m Fe_{92-m} C_8$, $Dy_2 Fe_{14} B$ made by MA and subsequent annealing
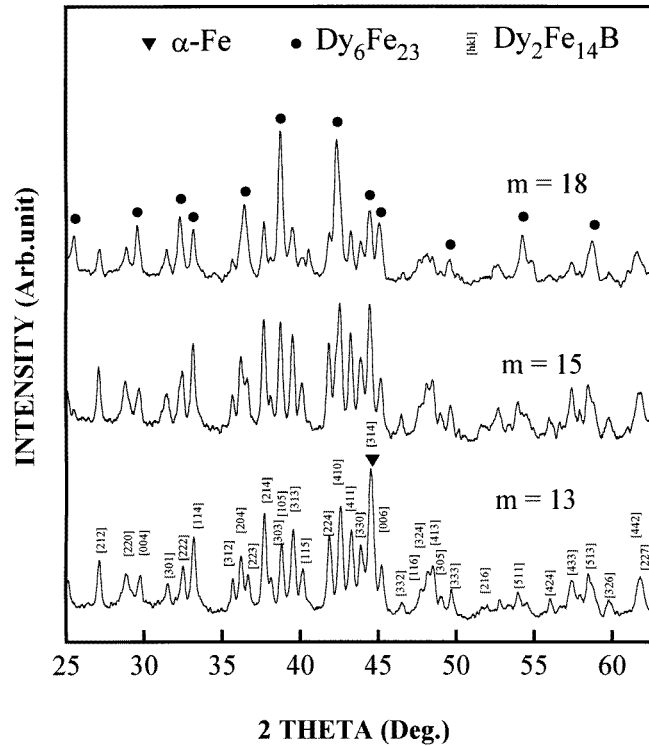
Figure 3. X-ray diffraction patterns of mechanically alloyed $Dy_m Fe_{92-m} B_8$ alloys annealed at 900 °C for 35 min.

has a fairly narrow composition range around $m = 15$. Dy content less than 14 at.% leaves a certain amount of α-Fe unreacted with Dy and C. In contrast to the formation of Dy-rich phase in Dy–Fe–C alloys, excessive Dy contents higher than 15 at.% cause the formation of the cubic structure $Dy_6 Fe_{23}$. Its amount increases also with the increment of Dy content. The Curie temperature of $Dy_6 Fe_{23}$ in the MA Dy–Fe–B alloy is 265 °C, which is the same as that of $Dy_6 Fe_{23}$ in Dy–Fe casting [8].

3.2. Magnetic properties

The dependence of coercivity on annealing temperature shows that the largest coercivity for the two series of alloys is achieved when annealed at 900 °C for 35 min. So the comparisons of magnetic properties are confined to the alloys under the same vacuum annealing at 900 °C for 35 min.

3.2.1. $Dy_m Fe_{92-m} C_8$ ($13 \leqslant m \leqslant 20$). Figure 5 presents the demagnetization curves of MA $Dy_m Fe_{92-m} C_8$ alloys annealed at 900 °C for 35 min. The coercivity has its maximum value of $_i H_c = 93$ kOe at $m = 18$ and falls down on both sides. The coercivity value of $Dy_{13} Fe_{79} C_8$ alloy is only 1.6 kOe due to the excessive amount of α-Fe and $Dy_2 Fe_{17} C_x$ present in it. The demagnetization curve presents a shoulder for the $m = 15$ alloy, which is caused by α-Fe in the alloy. Although $Dy_{15} Fe_{77} C_8$ alloy has much more Dy than the stoichiometric ratio in the $Dy_2 Fe_{14} C$ phase, the formation of more Dy-rich phase depletes
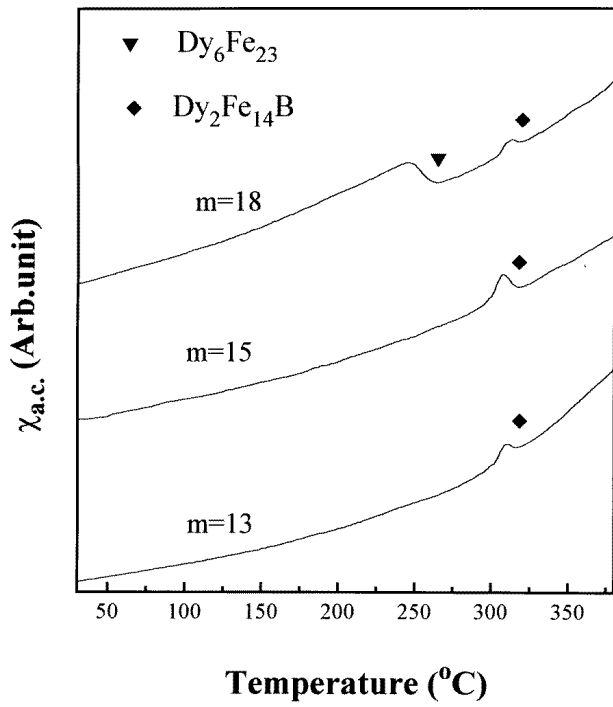
Figure 4. χ_{ac} against temperature of mechanically alloyed $Dy_mFe_{92-m}B_8$ alloys annealed at 900 °C for 35 min.
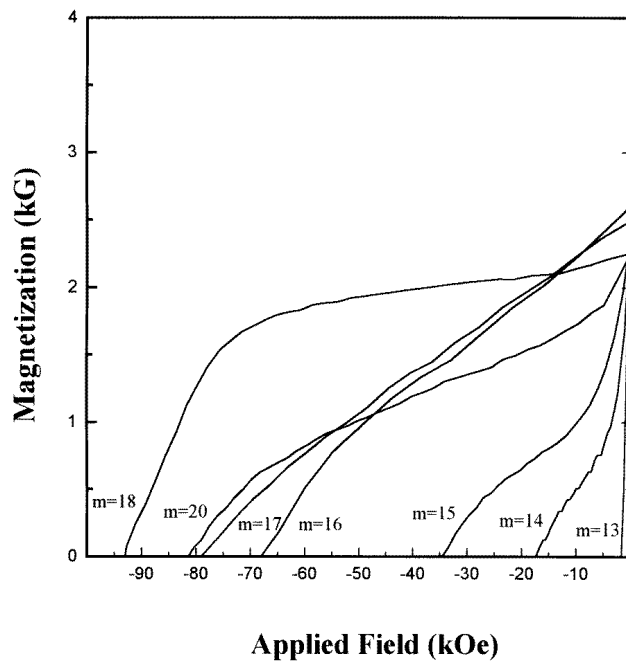

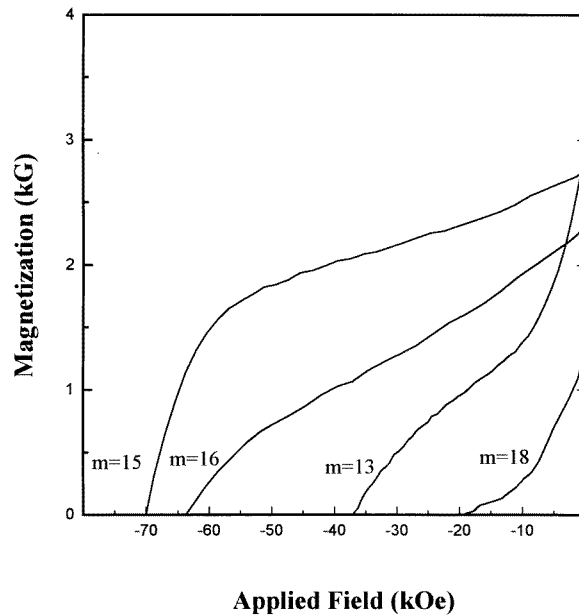**Figure 5.** Demagnetization curves of $Dy_mFe_{92-m}C_8$ alloys annealed at 900 °C for 35 min.

Figure 6. Demagnetization curves of $Dy_mFe_{92-m}B_8$ alloys annealed at 900 °C for 35 min.

the remaining material of Dy compared to the stoichiometric composition, leading to the formation of α-Fe.

From $m = 16$ to $m = 18$, no shoulder can be observed. Both the highest coercivity and rectangularity are achieved for $Dy_{18}Fe_{74}C_8$ alloy.

In a sintered Nd–Fe–B magnet, an fcc Nd-rich phase with lattice parameter of $a = 5.2$ Å is detected [9, 10]. This phase consists of nearly 95 at.% Nd and 5 at.% Fe which lies between the hard magnetic grains. Similarly, one may expect a thin Dy-rich phase layer covers the single-domain $Dy_2Fe_{14}C$ particles. From figures 1 and 2, one can conclude that the coercivity correlates directly to the amount of the Dy-rich phase (from $m = 16$ to $m = 18$). In other words, more Dy-rich phase brings about higher intrinsic coercivity. It is reasonable to infer that the Dy-rich phase is a non-magnetic or paramagnetic compound. More Dy-rich phase means more complete separation of $Dy_2Fe_{14}C$ grains, which decreases the coupling field between hard magnetic grains with random orientation, increases the nucleation field and the expansion field of reversed domain. All these factors constitute to increase the coercivity of Dy–Fe–C alloys with high content of Dy-rich phase. Excessive Dy content at $m = 19$ and $m = 20$ triggers the formation of $Dy_2Fe_{17}C_x$ again and spoils the intrinsic coercivity and the rectangularity of the demagnetization curves.

3.2.2. $Dy_mFe_{92-m}B_8$. Figure 6 demonstrates the demagnetization curves of MA $Dy_mFe_{92-m}B_8$ alloys annealed at 900 °C for 35 min. The intrinsic coercivity is enhanced by the increment of Dy content, reaches its maximum at $m = 15$ and decreases thereafter. α-Fe and Dy_6Fe_{23} are responsible for the dropping down of the intrinsic coercivity at the Dy-poor and the Dy-rich sides of composition respectively. From figure 3, one finds several weak peaks that do not belong to $Dy_2Fe_{14}B$, Dy_6Fe_{23} and Dy-rich phase, indicating the presence

of other types of secondary minor phase. It is hard to clarify the role of the minor phases in the intrinsic coercivity because the minor phases are too small to be indexed. The magnetic properties of the alloys are sensitive to microstructure modification introduced by the minor phases. In Dy–Fe–B alloys, no Dy-rich phase exists, so that enough Dy reacts with α-Fe and boron to form the $Dy_2Fe_{14}B$ compound. Thus higher coercivity is achieved for the $Dy_{15}Fe_{77}B_8$ alloy.

4. Conclusions

Mechanically alloyed and annealed Dy–Fe–C and Dy–Fe–B alloys have different composition windows for the formation of $R_2Fe_{14}X$ (X = B, C) phases. The $Dy_2Fe_{14}C$ compound can form within composition range of $15 \leqslant m \leqslant 18$. Dy content beyond this range causes the formation of $Dy_2Fe_{17}C_x$ with different Curie temperatures accompanying the tetragonal $Dy_2Fe_{14}C$ phase. Meanwhile, the composition range for the formation of $Dy_2Fe_{14}B$ is rather narrower. When $m \geqslant 16$, Dy_6Fe_{23} forms and when $m \leqslant 14$, a certain amount of α-Fe unreacted with Dy and C is left.

An fcc structure Dy-rich phase which might be non-magnetic or paramagnetic emerges in Dy–Fe–C alloys during the annealing process and its amount increases with the increment of Dy content. The homogeneous distribution of this phase separates the hard magnetic grains, resulting in higher coercivity. No Dy-rich phase is found in the Dy–Fe–B series of alloys. The largest coercivities obtained in the Dy–Fe–C and the Dy–Fe–B systems are 93 kOe and 70 kOe respectively.

Acknowledgments

References

[1] van Mens R, de Mooij D B and Buschow K H J 1988 *J. Appl. Phys.* **64** 5708
[2] Stadelmaier H H and Jang T S 1989 *IEEE Trans. Magn.* **MAG-25** 3423
[3] Liu N C and Stadelmaier H H 1987 *J. Appl. Phys.* **61** 3574
[4] Schultz L and Wecker J 1987 *Proc. 9th Int. Workshop on Rare Earth Magnets and their Application (Bad Soden)* ed C Herget and R Poerschke (Deutsche Physikalische Gesellschaft, Bad Honnef, FRG) p 301
[5] Pinkerton F E 1986 *J. Magn. Magn. Mater.* **54–57** 579
[6] Sagawa M, Hirosawa S, Tokuhara K, Yamamoto H, Fujimura S, Tsubokawa Y and Shimizu R 1987 *J. Appl. Phys.* **61** 3559
[7] Shen B G, Wang F W, Kong L S, Cao L and Zhan W S 1994 *J. Appl. Phys.* **75** 6523
[8] vander Goot A S and Buschow K H J 1970 *J. Less-Common. Met.* **21** 151
[9] Ramesh R, Chen J K and Thomas G 1987 *J. Appl. Phys.* **61** 2993
[10] Fidler J, Knoch K G, Kronmüller H and Schneider G 1989 *J. Mater. Res.* **4** 806